Published in final edited form as:
Development. 2008 November ; 135(21): 3599–3610. doi:10.1242/dev.025437.

An FGF autocrine loop initiated in second heart field mesoderm regulates morphogenesis at the arterial pole of the heart

Eon Joo Park[1,*], **Yusuke Watanabe**[2,*], **Graham Smyth**[3], **Sachiko Miyagawa-Tomita**[4], **Erik Meyers**[3], **John Klingensmith**[3], **Todd Camenisch**[5], **Margaret Buckingham**[2], and **Anne M. Moon**[1,6,7,†]

[1]Department of Neurobiology and Anatomy, University of Utah, Salt Lake City, UT 84112, USA.

[2]Department of Developmental Biology, CNRS URA 2578, Pasteur Institute, Paris 75015, France.

[3]Department of Cell Biology, Duke University, Durham, NC 27710, USA.

[4]Department of Pediatric Cardiology, Tokyo Women's Medical University, Tokyo 162-8666, Japan.

[5]Department of Pharmacology and Toxicology, University of Arizona, Tuscon, AZ 85721, USA.

[6]Department of Pediatrics, University of Utah, Salt Lake City, UT 84112, USA.

[7]Program in Human Molecular Biology and Genetics, University of Utah, Salt Lake City, UT 84112, USA.

Abstract

In order to understand how secreted signals regulate complex morphogenetic events, it is crucial to identify their cellular targets. By conditional inactivation of *Fgfr1* and *Fgfr2* and overexpression of the FGF antagonist sprouty 2 in different cell types, we have dissected the role of FGF signaling during heart outflow tract development in mouse. Contrary to expectation, cardiac neural crest and endothelial cells are not primary paracrine targets. FGF signaling within second heart field mesoderm is required for remodeling of the outflow tract: when disrupted, outflow myocardium fails to produce extracellular matrix and TGFβ and BMP signals essential for endothelial cell transformation and invasion of cardiac neural crest. We conclude that an autocrine regulatory loop, initiated by the reception of FGF signals by the mesoderm, regulates correct morphogenesis at the arterial pole of the heart. These findings provide new insight into how FGF signaling regulates context-dependent cellular responses during development.

Keywords

FGF; Heart development; Outflow tract; Second heart field; Autocrine signaling; Epithelial-mesenchymal transformation; Mouse

INTRODUCTION

Many congenital heart defects are caused by abnormal remodeling of the arterial pole of the heart, called the outflow tract (OFT). Cells are added to both poles of the heart from a second

†Author for correspondence (anne.moon@genetics.utah.edu).
*These authors contributed equally to this work

Supplementary material Supplementary material for this article is available at http://dev.biologists.org/cgi/content/full/135/21/3599/DC1

population of cells located in pharyngeal and splanchnic mesoderm dorsal to the heart tube, called the second heart field (SHF), which is crucial for the formation of the OFT (Buckingham et al., 2005). After looping of the heart, the myocardium secretes a specialized extracellular matrix (ECM) called the cardiac jelly that forms internal cushions; these cushions ultimately form the septa and the valves. The cushion jelly is invaded by endothelial cells lining the OFT myocardium that undergo an endothelial-to-mesenchymal transformation (EMT), and by a subset of neural crest cells called the cardiac neural crest (CNC) (Kirby, 2006). These events require BMP, TGFβ, WNT and semaphorin signaling from the OFT myocardium, in addition to proper cardiac jelly composition (Armstrong and Bischoff, 2004; High and Epstein, 2007). Thus, dysfunction of many different cell types and signaling pathways can contribute to abnormal OFT morphogenesis.

At midgestation, the OFT is remodeled by spiraling and fusion of the cushions to septate the OFT into the aorta and pulmonary artery; this occurs concurrent with rotation and alignment of the OFT relative to the ventricles. When alignment/rotation of the septated OFT is disrupted, transposition of the great arteries (TGA) or double-outlet right ventricle (DORV) occurs. Complete failure of OFT septation results in persistent truncus arteriosus (PTA), in which the primitive OFT (the truncus arteriosus) is not divided into the aorta and pulmonary artery. These defects disrupt the partitioning of blood flow required for adequate oxygenation and are lethal in mice and humans.

The importance of FGF8 signaling for heart development is clear. *Fgf8*-null mutants die at gastrulation (Sun et al., 1999). However, *Fgf8* hypomorphs survive to birth with OFT septation and alignment/rotation defects (Abu-Issa et al., 2002; Frank et al., 2002). Conditional mutagenesis has been used to determine the spatiotemporal requirements for *Fgf8* function in different aspects of OFT morphogenesis (Ilagan et al., 2006; Macatee et al., 2003; Park et al., 2006). Mutation of *Fgf8* in mesodermal heart precursors in the primitive streak can prevent OFT formation and cause embryonic death; however, survivors display OFT rotation/alignment defects. When *Fgf8* is inactivated later in development, in OFT precursors in the SHF and in pharyngeal endoderm, the mutants survive, but all have PTA (Park et al., 2006). Although *Fgf10* is expressed in the SHF, and *Fgf15* in multiple tissues in the pharyngeal arches, only *Fgf15*-null mutants have OFT defects (Marguerie et al., 2006; Vincentz et al., 2005).

We have made progress in identifying the sources and FGF ligands required for OFT development, but their cellular targets remain unknown. The accepted paradigm is that FGFs signal in a paracrine manner to target cells via the FGF receptor tyrosine kinases (RTKs, FGFR1-4). Mitogenic assays suggest that ligand-receptor preferences exist (Zhang, X. et al., 2006), but overlapping expression patterns and ablation studies reveal functional redundancy (Sun et al., 2002). Variations in ECM composition are likely to modify ligand-receptor interactions and signaling in a context-dependent manner. Thus, defining functionally relevant ligand-receptor interactions on target cells that regulate specific morphogenetic events in vivo is an important endeavor.

Some insight into these crucial in vivo interactions can be obtained by comparing phenotypes of FGF receptor and ligand mutants. *Fgfr1*-null mutants die at gastrulation (Deng et al., 1994), whereas *Fgfr2*-null mutants die post-implantation (Arman et al., 1998). Previous manipulations of *Fgfr1/2* function that bypass lethality reveal crucial roles for these receptors in many processes and suggest that they are important for cardiovascular development (Marguerie et al., 2006; Moon et al., 2006; Trokovic et al., 2003). By contrast, *Fgfr3* and *Fgfr4* double-null mutant mice survive without cardiovascular defects (Weinstein et al., 1998).

Here, we conditionally inactivate *Fgfr1* and *Fgfr2* and conditionally overexpress sprouty 2 (*Spry2*, which encodes an FGF signaling antagonist) in different cell types to identify the direct cellular targets of FGF signals required for OFT remodeling. Our results reveal that although published evidence points to CNC and/or OFT endothelial cells as crucial paracrine targets (Kirby, 2006; Presta et al., 2005), disrupting FGF signaling to these populations does not prevent OFT remodeling. Rather, we show that interrupting autocrine FGF signaling in SHF mesoderm causes an OFT myocardial secretory defect; this secondarily perturbs endothelial EMT and CNC invasion in association with altered BMP and TGFβ signaling. Graded alterations in OFT development with varying FGF receptor gene dosage reveal a marked sensitivity to FGF signaling in target cells. We conclude that the specialized secretory and signaling properties of the primitive OFT that drive OFT morphogenesis are regulated by an autocrine FGF signaling loop.

MATERIALS AND METHODS

Genetically engineered mice

Construction and activity of the *Fgfr1*, *Fgfr2* and *Fgf8* conditional alleles (denoted as 'c' alleles throughout) were described previously (Park et al., 2006; Trokovic et al., 2003; Xu et al., 2002; Yu et al., 2003). Generation and characterization of *Wnt1Cre*, *Ap2αIRESCre*, *Pax3Cre*, *Mesp1Cre*, *Isl1Cre*, *Tie2Cre* (*Tie2* is also known as *Tek* — Mouse Genome Informatics), *Foxa2MCM* and *Spry2-GOF* alleles have also been reported previously (Basson et al., 2008; Danielian et al., 1998; Engleka et al., 2005; Jiang et al., 2000; Kisanuki et al., 2001; Macatee et al., 2003; Park et al., 2006; Park et al., 2008; Saga et al., 2000). The *Isl1Cre* and *Mesp1Cre* males used to generate the mutants are in mixed backgrounds: *Isl1Cre* is 50% C57Bl6 and 25% each BlSw and Sv129; *Mesp1Cre* is 50% C57Bl6 and 25% each ICR and SV129. These males were bred to *Fgfr1/2* conditional females that are in a complex mixed background (including C57Bl6, Sv129 and others). Thus, the embryos arising from each cross are outbred. To generate the *Fgfr1;IRESCFP* and *Fgfr2;IRESYFP* alleles in mice, we inserted *IRES;FP;frt*-flanked neomycin cassettes into the 3′ untranslated regions of each gene upstream of the polyadenylation signal. All experiments were in accordance with institutional and national guidelines and regulations.

OFT explant culture and co-culture on collagen gels

Collagen gels were made as previously described (Camenisch et al., 2002). OFT segments were isolated, opened to expose endocardium, placed on the gel and allowed to attach for 12 hours without addition of culture media. Then 1×M199 containing 1% fetal bovine serum (FBS), 0.01% insulin-transferrin-selenium (ITS) and 1% PenStrep (Gibco-BRL) was added and the explants cultured for 48 hours. For co-cultures, $Fgf8^{c/c}$;$Rosa26^{lacZ/lacZ}$ and $Fgf8^{c/c}$ females were bred with $Fgf8^{+/-}$;*Isl1Cre* males to obtain labeled *Fgf8;Isl1Cre* mutants and controls. OFTs from mutants and controls were placed immediately adjacent to one another. Explants were fixed and stained using standard protocols.

Immunohistochemistry and in situ hybridization

YFP and CFP detection was performed using rabbit anti-GFP and Texas Red-conjugated anti-rabbit secondary antibodies (Molecular Probes) on cryosectioned specimens. Anti-phosphohistone H3 (Ser10, Cell Signaling Technology), anti-ISL1 (Developmental Studies Hybridoma Bank), anti-AP2α (TCFAP2α — Mouse Genome Informatics) (3B5, Developmental Studies Hybridoma Bank), anti-phosphorylated (p) ERK1/2 and SMAD1/5/8 (Cell Signaling Technology) and FITC-conjugated anti-mouse secondary (Molecular Probes) antibodies were used. In situ hybridization was performed with a standard protocol (Grove et al., 1998) and digoxigenin-labeled antisense RNA probes. Alkaline phosphatase and β-

galactosidase staining were performed using published protocols (Frank et al., 2007; Lobe et al., 1999).

Preparation of RNA and cDNA for microarray and quantitative RT-PCR

E9.5 OFTs were dissected and stored in RLT buffer (Qiagen) at −80°C. Seven specimens of each genotype (*Fgf8*$^{c/+}$, control; *Fgf8*$^{c/-}$*;Isl1Cre*, mutant) were pooled to generate each sample. Total RNA was extracted from four samples (RNeasy Micro Kit, Qiagen). Agilent two-color LRILAK labeling, the Agilent two-color GE hybridization/wash protocol, and the Agilent 5-micron XDR scanning protocols were carried out by the University of Utah Microarray Core Facility. RNA (100 ng) was reverse-transcribed to cDNA using the SuperScript III First-Strand Synthesis System (Invitrogen). Quantitative RT-PCR was performed with iQ SYBR Green Supermix on the iCycler system (Bio-Rad). *Hprt* transcript was used as the reference level.

Microarray data analysis

This experiment was run in quadruplicate on Agilent mouse whole-genome expression arrays. The array image data were quantitated using Agilent Feature Extraction software (version 9.5.1.1). Subtle intensity-dependent bias was corrected with LOWESS normalization, with no background subtraction. Statistical analysis of normalized log-transformed data was performed in Gene Sifter (www.genesifter.net). Differentially expressed transcripts were defined (adjusted for multiple testing using the Benjamini and Hochberg method) as $P<0.05$. Spots with an intensity below background were removed prior to statistical analysis. Data were hierarchically clustered with Spotfire (TIBCO) and heat maps for selected genes were generated. Log-transformed, normalized gene intensity data were clustered by the UPGMA method; Pearson's correlation was the distance metric.

RESULTS

Neural crest invasion and endothelial cell EMT in the OFT cushions fail in *Fgf8;Isl1Cre* mutants

Loss of *Fgf8* function in the SHF and pharyngeal endoderm in *Fgf8*$^{c/-}$*;Isl1Cre* conditional mutants (hereafter referred to as *Fgf8;Isl1Cre*) causes PTA (Park et al., 2006). We found that the OFT cushions of these mutants contain markedly less cardiac jelly and fewer mesenchymal cells than controls (Fig. 1A-H; see Fig. S1 in the supplementary material). The mutant OFTs were short and aberrantly angulated.

To distinguish the sources of cushion mesenchymal cells at early stages of OFT septation, we used the conditional *Rosa26*^{lacZ} reporter (Soriano, 1999) and *Tie2Cre* (Kisanuki et al., 2001) to label endothelial cells (which constitute the endocardial lining of the OFT). *Tie2Cre* activity was uniform in the OFT endothelium by E8.25 (Fig. 1I-K). This experiment shows that most cells in the proximal cushions at E11.5 are of endothelial origin; although CNC cells have invaded the distal OFT, few have as yet migrated into the proximal cushions (Fig. 1E,G,J and data not shown). We explanted proximal cushions from E9.25 *Rosa26*^{lacZ}*;Tie2Cre* embryos onto collagen gels and found that the cells from the explant that undergo EMT to invade and migrate into the gel are β-galactosidase-positive (Fig. 1K,L), confirming their endothelial origin. Since the OFT cushions of *Fgf8;Isl1Cre* mutants were hypoplastic along their entire proximodistal extent (the proximal cushions were both thinner and had fewer cells, whereas the distal cushions were thinner but with no change in cell density) (Fig. 1; see Fig. S1 in the supplementary material), both endothelial and CNC cells are affected in these mutants.

OFT remodeling is independent of direct FGF signaling to cardiac neural crest and endothelial cells

In order to understand how FGF8 regulates endothelial and CNC invasion of the OFT cushions, we sought to identify the direct cellular targets of FGF8 and of other FGF ligands required for OFT remodeling. The overlapping phenotypes reported in different types of *Fgf8*, *Fgfr1* and *Fgfr2* mutant mice suggest that FGF8 signals through these receptors during embryogenesis. We first determined which cells within the pharyngeal arches and SHF express these receptors. We generated novel alleles to fluorescently label cells expressing *Fgfr1* and *Fgfr2* by targeting an IRES (internal ribosome entry site) and CFP to *Fgfr1*, and an IRES and YFP to *Fgfr2*. We detected ubiquitous expression of both receptors in the anterior embryo, including all cells in the pharynx at E8.5-9.5 (see Fig. S2 in the supplementary material), with variable levels of signal in different cell types.

Based on these expression data, we systematically ablated these receptors in the mesodermal precursors of the OFT in the SHF and in other pharyngeal tissues. We assayed whether ablation of *Fgfr1* and/or *Fgfr2* in a tissue phenocopies the OFT septation defects seen in *Fgf8;Isl1Cre* mutants, or the OFT alignment defects seen in *Fgf8;Mesp1Cre* mesodermal mutants (Park et al., 2006). Each of the Cre drivers used has an onset of Cre-mediated recombination in the desired tissue that is prior to the requisite window of FGF8 signaling at E8.5 (8- to 10-somite stage) that we previously identified for OFT remodeling (Park et al., 2006).

In complementary experiments, we employed conditional *Spry2* gain-of-function (*Spry2-GOF*) to inhibit ERK phosphorylation downstream of activated RTK signaling, including that of FGFRs (Hanafusa et al., 2002). After Cre-mediated recombination, the *Spry2-GOF* transgene constitutively expresses *Spry2* (Fig. 2) (Basson et al., 2008). Activation resulted in markedly increased production of *Spry2* mRNA relative to controls (Fig. 2F,H), and effective antagonism of FGF signaling was evident by decreased ERK activation (Fig. 2J,J') and decreased expression of the FGF8 target gene *Erm* (*Etv5*) (Fig. 2L) (Park et al., 2006; Raible and Brand, 2001; Roehl and Nusslein-Volhard, 2001). *Pea3* (*Etv4*) expression was also decreased at E8.5 (not shown).

To test whether CNC cells are direct targets of the FGF signaling required for OFT remodeling, we used the well-characterized *Wnt1Cre* and *Ap2αIRESCre* drivers to ablate *Fgfr1* and *Fgfr2* function in premigratory neural crest, and in premigratory neural crest and pharyngeal ectoderm, respectively (Jiang et al., 2000; Macatee et al., 2003). Surprisingly, ablation of either receptor, independently or in combination, did not disrupt OFT remodeling (see Table S1 in the supplementary material). As expected, these embryos had disrupted craniofacial development (see Fig. S3 in the supplementary material). Furthermore, when we overexpressed *Spry2* in neural crest, 100% of mutants had abnormal craniofacial structures but normal OFT morphology (see Table S1 and Fig. S3 in the supplementary material). This indicates that OFT septation is independent of FGF signaling directly to CNC. PDGF signaling, which is known to occur in neural crest (Richarte et al., 2007), is therefore not a major target of inhibition by sprouty 2 in these cells.

Extensive published evidence demonstrates that FGFs stimulate migration and invasiveness of endothelial cells (Auguste et al., 2003). Since the proximal OFT cushions of *Fgf8;Isl1Cre* mutants have few endothelium-derived mesenchymal cells, we examined the ability of endothelial cells from *Fgf8;Isl1Cre* mutants to migrate from an explanted OFT, undergo EMT, and invade a collagen gel. Remarkably, 100% of mutant OFT explants exhibited a dramatic failure of EMT (Fig. 3B, n=11). In control explants, only an occasional cell appeared rounded and on the gel surface (Fig. 3A), whereas in the mutants, the few cells that migrated away from

the explant were rounded up on the surface or fragmented into debris (Fig. 3B). For quantitation of these findings, see Fig. S4 in the supplementary material.

We then tested whether loss of FGF signaling directly to endothelial cells causes OFT defects using *Tie2Cre* (Kisanuki et al., 2001) to ablate *Fgfr1* and *Fgfr2*. *Tie2Cre* conditional mutants survived and had normal OFTs (see Table S1 in the supplementary material; data not shown). This suggests that the endothelial EMT defect seen in *Fgf8;Isl1Cre* mutants in vivo (Fig. 1), and in explants (Fig. 3), is endothelial cell-non-autonomous. To test this, we co-cultured *Fgf8;Isl1Cre* mutant explants adjacent to those from controls. To identify the origin of invading cells in co-culture, we used the conditional $Rosa26^{lacZ}$ line and *Isl1Cre* to label endothelial cells from control explants, or carried the $Rosa26^{lacZ}$ allele in the females used to generate conditional mutant explants [the *Isl1Cre* expression domain includes OFT endothelium (Park et al., 2006) (data not shown)]. We found that control explants rescued the ability of *Fgf8;Isl1Cre* mutant endothelial cells to undergo EMT (Fig. 3D,E), with no adverse effect of *lacZ* expression in controls (Fig. 3C). In addition to confirming that the EMT defect in *Fgf8;Isl1Cre* mutants is not due to primary endothelial dysfunction, this finding suggests that the essential defect in the mutant OFTs resides within the myocardium itself.

SHF mesoderm is a direct target of FGF signals required for OFT remodeling

Based on the co-culture results, we predicted that loss of FGF signaling to mesodermal precursors of the OFT would phenocopy the defects of *Fgf8* conditional mutants. We ablated *Fgfr1* and *Fgfr2* using the mesoderm-specific driver *Mesp1Cre*. This driver is active in the anterior primitive streak and ablates gene function in all myocardial and endocardial precursors (Park et al., 2006; Saga et al., 1999). Fourteen percent of $Fgfr1^{c/c};Fgfr2^{+/+};Mesp1Cre$ mutants had alignment defects (TGA and DORV, Table 1). The frequency of alignment defects increased to 40% with decreasing *Fgfr1/2* gene dosage in $Fgfr1^{c/c};Fgfr2^{c/+};Mesp1Cre$ mutants (Fig. 4C, Table 1). Normally, persistence of myocardium in the right ventricular subvalvar outflow region (called the conus, derived from the SHF) and regression of this myocardium on the left side causes the pulmonary valve to ultimately reside above (distal to the ventricle) the aortic valve (Fig. 4A'). Hypoplasia of the right conus in *Fgfr1/2* mutants was apparent externally as a flattening of this region (Fig. 4C), and resulted in a side-by-side valve position (Fig. 4C'). Linkage of *Mesp1* and *Fgfr2* on chromosome 7, with a predicted recombination frequency of 23%, prevented analysis of large numbers of $Fgfr1^{c/+};Fgfr2^{c/c};Mesp1Cre$ and $Fgfr1^{c/c};Fgfr2^{c/c};$ *Mesp1Cre* mutants. However, there were no OFT defects in the $Fgfr1^{c/+};Fgfr2^{c/c};Mesp1Cre$ mutants we obtained (Table 1). By contrast, four out of five of $Fgfr1^{c/c};Fgfr2^{c/c};Mesp1Cre$ mutants had PTA type III, a severe grade of PTA in which the OFT is unseptated along its entire proximodistal extent (Fig. 4D,D'). The truncal OFT valve was also abnormally aligned. Since the incidence and severity of OFT defects increase with decreasing *Fgfr1/2* gene dosage in the mesoderm, the ability to align and septate the OFT depends on the amount of FGF signaling received by these cells. Our data also indicate that the dominant receptor transducing the required signals in this process is FGFR1, as FGFR2 has only partial compensatory activity.

Our observation of 100% type III PTA in *Fgf8;Isl1Cre* ligand mutants suggests that FGF8 signaling to mesoderm and endoderm might have additive influences on OFT remodeling. Indeed, ablation of *Fgfr1* and *Fgfr2* in the *Isl1Cre* domain [which encompasses both endoderm and SHF mesoderm at E8.0 (Park et al., 2006)] increased the frequency of type III PTA to 100% in $Fgfr1^{c/c};Fgfr2^{c/c};Isl1Cre$ mutants (Table 1), as compared with 66% in mesoderm-only double mutants. Defects in $Fgfr1^{c/c};Fgfr2^{c/+};Isl1Cre$ mutants were also more severe than those in their mesoderm-only counterparts because proximal OFT septation frequently failed, resulting in type I PTA (Fig. 4G, Table 1). In this form of PTA (which is common in human patients), there is a single truncal valve, but the distal OFT is septated (Fig. 4G,G'). Consistent

with our hypothesis that FGFR1 is the principal receptor, *Fgfr1$^{c/+}$;Fgfr2$^{c/c}$;Isl1Cre* mutants had milder defects than *Fgfr1$^{c/c}$;Fgfr2$^{c/+}$;Isl1Cre* mutants (Fig. 4F, Table 1).

These data suggest that FGF signaling to the pharyngeal endoderm plays a role in OFT remodeling. We used a novel Cre driver, *Foxa2IRES mER-Cre-mER* (Park et al., 2008), to ablate *Fgf8* or *Fgfr1* and *Fgfr2* in pharyngeal endoderm by E8.0 and test whether independent effects of endodermal FGF signaling on OFT septation could be detected. Although loss of endodermal receptor function disrupts vascular development (E.J.P. and A.M.M., unpublished), endodermal ligand and receptor mutants survived to birth and had normal OFTs (see Table S1 in the supplementary material).

Antagonism of FGFR-mediated signaling in SHF mesoderm in *Spry2-GOF;Mesp1Cre* embryos caused phenotypes consistent with the receptor ablation results: 75% of these mutants had heart defects, most of which were arterial pole abnormalities (PTA and DORV, Fig. 5A-I, Table 1). Additionally, as in *Fgf8;Isl1Cre* mutants (Fig. 1), the OFTs of E9.5 *Spry2-GOF;Mesp1Cre* mutants were significantly shorter than in controls and were at an obtuse angle to the right ventricle (Fig. 5J-O and data not shown). *Wnt11* transcripts in the OFT myocardium were reduced in E9.5 *Spry2- GOF;Mesp1Cre* mutants (Fig. 5J,K) and *Bmp4* expression was also notably downregulated in the OFT and SHF (Fig. 5L,M). Both *Spry2-GOF;Mesp1Cre* and FGFR mutants phenocopied the early defects in endothelial EMT and CNC invasion seen in *Fgf8;Isl1Cre* mutants (Fig. 5P,Q; see Fig. S5 in the supplementary material). Reduction in EMT was demonstrated in *Spry2-GOF;Mesp1Cre* mutant explants (Fig. 5R,S), similar to that shown for *Fgf8;Isl1Cre* mutants (Fig. 3A,B). Proliferation of ISL1-expressing cells in the SHF and OFT myocardium was significantly decreased in *Spry2-GOF;Mesp1Cre* mutants at multiple stages (Fig. 5T-V and data not shown); this is also seen in *Fgf8* mutants (Park et al., 2006). Mesodermal *Spry2-GOF* phenotypes are similar to those of the FGFR mutants; since SPRY2 inhibits signaling downstream of other RTKs, this demonstrates the primacy of FGF signaling in SHF mesoderm for subsequent OFT morphogenesis. However, the effects on *Wnt11* and *Bmp4* transcripts suggest that downstream modulation of other signaling pathways is likely to affect CNC and endothelial cell behavior in the OFT. Detection of these OFT markers, albeit at a lower level, demonstrates that OFT progenitors continue to be added from the SHF when FGF signaling is compromised.

Crucial signaling pathways that regulate EMT and cardiac neural crest behavior are disrupted by loss of FGF signaling in the SHF and pharyngeal endoderm

In order to examine downstream effects of loss of FGF8 on myocardial signaling, we examined gene expression in isolated E9.5 OFTs from *Fgf8;Isl1Cre* mutants and controls using genome-wide microarray analysis. This timing allowed us to examine myocardial and endocardial gene activity at the onset of endocardial EMT and CNC invasion. In the FGF pathway (Fig. 6A), few genes were dysregulated greater than 2-fold. Expression of the known FGF8 target genes *Pea3* and *Erm* was significantly decreased, as expected. Reductions seen in the expression of genes encoding FGF counter-regulatory factors [sprouty, Spred, *Il17rd* (*Sef*) and Dusp genes] were similar.

When FGF signaling to the SHF and endoderm was perturbed, there were striking changes in the level of transcripts of components of the BMP, TGFβ and semaphorin/plexin pathways, which are known to be essential to both endocardial EMT and CNC survival and invasion of the OFT cushions (Barnett and Desgrosellier, 2003; High and Epstein, 2007) (Fig. 6B,D,E and data not shown). Quantitative RT-PCR confirmed these findings and revealed that the array frequently underestimated the magnitude of the expression changes (see Table S2 in the supplementary material). *Bmp4* and *Bmp2* transcripts were decreased, as was the expression of genes in the *Bmp4* synexpression group (Karaulanov et al., 2004), including the transcriptional effectors *Msx1* and *Msx2*, and target genes with roles in OFT endocardial EMT

(*Has2*, *Gata4*, *Tbx3*, *Twist1*, *Snai1*) (Liu et al., 2004). Transcripts for some BMP antagonists (noggin, *Bambi*) and inhibitory Smads (*Smad6*, *Smad7*) were also decreased, and increased expression of the BMP antagonist gremlin 2 in the face of decreased *Bmp4/2* would further decrease BMP signaling. *Tgfb1* and *Tgfbr1* were also downregulated, together with *Tgfbrap1*, a protein induced by TGFβ that transmits signal from TGFβ receptors to SMAD2 and 4 (Wurthner et al., 2001).

BMP and TGFβ signaling regulate, and are modulated by, ECM composition. We found altered expression of genes encoding structural and signal-modulating ECM components. These included: *Has2*, a synthetic enzyme for hyaluronic acid, which is a major component of the cardiac jelly required for EMT (Camenisch et al., 2002); latent TGFβ-binding protein 1 (*Ltbp1*), a regulator of TGFβ bioavailability required for OFT septation (Todorovic et al., 2007); and the proteoglycans decorin (*Dcn*), biglycan (*Bgn*) and versican (*Vcan*; *Cspg2*), which influence the fibrous structure of collagen in the ECM and its physical interaction with cells, as well as the bioavailability and cellular responses to TGFβ and BMPs (Fig. 6B) (Macri et al., 2007).

Altered expression of these BMP/TGFβ pathway genes disrupted the activity of effector SMADs in the OFT cushions. The number of cells with detectable nuclear phosphorylated R-SMAD1/5/8 in the OFT endothelium and subendothelial mesenchyme of *Fgf8;Isl1Cre* and *Spry2-GOF;Mesp1Cre* mutants at E9.5 was dramatically decreased (Fig. 6G,I,I'). Our results clearly demonstrate that loss of FGF signaling negatively regulates signaling pathways that control EMT and CNC invasion of the OFT cushions.

DISCUSSION

In order to dissect how intercellular signaling regulates the complex cellular behaviors required for normal morphogenesis, it is crucial to identify not only the sources of the signals, but their cellular targets. In this way, we can discover immediate events and direct regulatory interactions in the target cells and distinguish them from secondary processes. In this study, we show that contrary to expectations, neural crest and endothelium are not the paracrine targets of the FGF signals that arise in SHF mesoderm and pharyngeal endoderm and are required for correct OFT formation, alignment and septation. Rather, we find that autocrine FGF signaling within the mesoderm of the SHF is absolutely required for septation of the OFT, and that signaling to the pharyngeal endoderm, although not independently required, has an additive function. Our data show that loss of FGF signaling within SHF mesoderm causes primary dysfunction of its derivatives in the OFT myocardium, evident by decreased production of cardiac jelly and dysfunction of pivotal signaling pathways from the myocardium to endothelium and CNC. Our results are consistent with those presented in a companion study (Zhang et al., 2008), in which ablation of the FGFR adaptor protein FRS2α (FRS2 — Mouse Genome Informatics) in the SHF and pharyngeal endoderm (but not neural crest or endothelium) causes arterial pole defects.

In our studies, FGFR gene ablation and *Spry2* gain-of-function obtained with *Mesp1Cre* occur not only in mesodermal precursors of the OFT in the SHF, but also in their derivatives. However, *Fgf8* ablation using Cre drivers with different temporal onset in the mesoderm (as it emerges from the primitive streak, at the crescent stage, when the SHF cells reside in the splanchnic mesoderm, or when SHF derivatives have already accrued to the heart) indicate that OFT defects only occur if *Fgf8* function is ablated at or before the crescent stage (Brown et al., 2004; Ilagan et al., 2006; Park et al., 2006). This temporal window indicates that the required FGF/FGFR signaling event occurs in the mesodermal precursors of the OFT in the SHF. Similar temporal requirements were identified for FRS2α-mediated signaling (Zhang et al., 2008). Furthermore, decreased cell proliferation, increased apoptosis and alterations in the

expression of *Isl1* and known FGF8 target genes are already marked in the SHF mesoderm of *Fgf8;Mesp1Cre* and *Fgf8;Isl1Cre* mutants by the 5- to 8-somite stage (Park et al., 2006); decreased proliferation is also striking in *Spry2-GOF;Mesp1Cre* embryos (Fig. 5), all of which point to primary effects on the progenitor cell population resulting in decreased OFT size and other defects.

An NKX2.5-BMP2/SMAD1 negative-feedback loop has been documented in the SHF in which diminution of BMP2/SMAD1 signaling increases progenitor cell proliferation and myocardial specification (Prall et al., 2007). Notably, *Fgf8* function was preserved in this system. Our findings suggest that BMP4/FGF8 participate in a different regulatory pathway because compromising FGF signaling resulted in decreased proliferation in the SHF associated with decreased *Bmp4* transcript levels in the SHF and reduced BMP signaling in the OFT. Indeed, differences between BMP2 and BMP4 function in the context of myocardial progenitor specification/proliferation, and in the OFT itself, have been documented (Armstrong and Bischoff, 2004; Klaus et al., 2007; Ma et al., 2005). In addition to effects on BMP signaling, which may affect the recruitment of differentiating myocardial cells (Waldo et al., 2001), we show that disrupted FGF signaling leads to reduced expression of *Wnt11* in OFT myocardium (Fig. 5), which was also seen in our microarray analysis (not shown), consistent with previous observations on *Fgf8;Isl1Cre* mutants (Park et al., 2006). Perturbation of non-canonical WNT11 signaling in the myocardium affects OFT development and interferes with *Tgfb2* transcription and ECM composition (Zhou et al., 2007).

The cushion defects in our FGF mutants focused our attention on the recruitment of neural crest. CNC cells do not arrive in the pharynx until ~xsE9.0. Thus, our finding that these cells are not the direct target of the early FGF signals is consistent with the temporal window identified using FGF ligand mutants in the SHF (Ilagan et al., 2006; Park et al., 2006). Although we did not specifically rule out a role for *Fgfr3* or *Fgfr4* in CNC during OFT remodeling, *Fgfr3/4* mutants have no cardiovascular defects (Weinstein et al., 1998). *Spry2-GOF* expression in these cells would antagonize signal transduction downstream of all four FGFRs, and *Spry2-GOF* neural crest cells have normal OFTs. Factors that antagonize SPRY2 activity could also influence the phenotype of these mutants. However, in an accompanying report, Zhang et al. show that ablation of *Frs2α* in CNC does not disrupt OFT development (Zhang et al., 2008), which is consistent with our findings. Indeed, the severe OFT defects in *Mesp1Cre* and *Isl1Cre* receptor mutants, in which *Fgfr1/2* function remains intact in CNC, indicate that disrupted FGF signaling to CNC is not required to generate these phenotypes.

Several lines of evidence indicate that secondary effects on CNC after loss of FGF signaling in the SHF play a role in the OFT phenotypes obtained in our mesodermal FGFR and *Spry2* gain-of-function mutants. The finding of aortic arch malformations in these mutants (Figs 4 and 5), but not in the neural crest conditional mutants (see Fig. S3 in the supplementary material), is consistent with downstream effects on neural crest. Excessive neural crest apoptosis is observed in *Fgf8* mutants (Ilagan et al., 2006;Macatee et al., 2003;Park et al., 2006), and *Spry2-GOF;Mesp1Cre* mutants have decreased neural crest *Crabp1* expression. Aortic arch defects have also been shown to be the result of secondary neural crest dysfunction due to *Tbx1* loss-of-function in the mesoderm of the SHF (Xu et al., 2004;Zhang, Z. et al., 2006). BMP and TGFβ signaling are essential for CNC invasion of the OFT cushions and for pharyngeal arch artery development (High and Epstein, 2007;Liu et al., 2004;Stottmann et al., 2004); the changes that we document in these pathways in the face of compromised FGF signaling will impact these processes. Modifications to ECM components, which also affect BMP/TGFβ signaling (Macri et al., 2007), further contribute to effects on the neural crest. In addition to the ECM and other signaling defects discussed above, transcription of *Acvr1* (*Alk2*), semaphorin 3c, plexin A3 and neuropilin 2 is decreased in *Fgf8;Isl1Cre* mutants (not shown). Each of these proteins critically impacts CNC function (High and Epstein, 2007).

Neural crest cells modulate FGF8 signaling in the pharynx and influence not only the addition of myocardium to the OFT from the SHF (Hutson et al., 2006), but also the contractile and secretory function of the myocardium itself, including its ability to produce cardiac jelly (Stottmann et al., 2004; Waldo et al., 1999). Thus, in affected *Fgf8*, FGFR and *Spry2* gain-of-function mutants, initial myocardial dysfunction and subsequent abnormal CNC behavior might interact in a cycle that progressively impairs OFT morphogenesis.

Since FGFR ablation in the endothelial precursors of the OFT endocardium does not perturb OFT remodeling, and EMT defects in *Fgf8;Isl1Cre* mutants can be rescued by wild-type myocardium, direct signaling between FGF ligands produced by the SHF and the endocardium is not required for OFT septation. Furthermore, ablation of *Frs2α* in the endothelium does not disrupt OFT morphogenesis (Zhang et al., 2008). However, defects in the expression of ECM components and signal modulators downstream of the BMP/TGFβ pathways provide insight into the molecular basis of the secondary endothelial dysfunction we observe (Barnett and Desgrosellier, 2003; Liu et al., 2004). Effects on these signaling pathways resulting from loss of FGF8 compromise the expression of numerous target genes with roles in endocardial EMT (*Has2*, *Gata4*, *Tbx3*, *Twist1*, *Snai1*) (Armstrong and Bischoff, 2004; Liu et al., 2004). TGFβi (TGFβ induced) stimulates endothelial migration by altering the structure of VE-cadherin intercellular junctions and integrin activity (Ma et al., 2008), and its downregulation might contribute to defective EMT in the mutant OFT.

In contrast to the paradigm of paracrine signaling established in other tissues, our data show that in the SHF, the cellular source of the ligand (signal) is also the target. Such an autocrine pathway can be easily understood in terms of a feedback loop that maintains FGF production within a tight range (E.J.P. and A.M.M., unpublished), which is crucial for FGF8 function (Hutson et al., 2006). Secondary effects on other signaling pathways that we observe may also be integrated into this regulatory loop. *Fgf8* and FGFR mutant analyses establish that the autocrine pathway not only regulates survival and proliferation of SHF cells (a common response to FGFs), but also the secretory and signaling capacities of their derivatives in the OFT (this study) (Zhang et al., 2008; Ilagan et al., 2006; Park et al., 2006). The few transcriptional targets of the PEA3 family of FGF8 effector proteins thus far identified are ECM components, ECM-modifying enzymes and cell adhesion molecules (de Launoit et al., 2006), suggesting that an autocrine pathway might provide a means of regulating the ECM and microenvironment to ensure uniform signal reception and response within a specialized cell population. Our findings are of biomedical importance, not only in the context of understanding the causes of congenital malformations of the OFT, but also because the crucial role we demonstrate for an autocrine FGF signaling pathway has broad implications for understanding fundamental properties of FGF signaling in different developmental and pathological contexts.

Supplementary Material

Refer to Web version on PubMed Central for supplementary material.

Acknowledgments

We thank C. Deng, J. Rossant, D. Ornitz, G. Martin, Y. Saga, J. Epstein and S. Evans for mouse lines; Brett Milash and the University of Utah Microarray Core; K. Thomas, M. Stevens and S. Vincent for critically reading the manuscript; and M. Stevens, D. Broka, E. Pecnard and C. Bodin for technical assistance. Y.W. and M.B. thank members of their lab, N. Duval, C. St Clement, R. Kelly and S. Zaffran for helpful discussions. S.M.-T. was supported by the Naito Foundation; Y.W. and M.B.'s lab by the E.U. Integrated Project 'Heart Repair' (LHSM-CT2005-018630), the Pasteur Institute and the CNRS; E.M. and J.K.'s lab by NIH HDO4803; and E.J.P. and A.M.M.'s lab by NIH/NICHD, AHA and the University of Utah Program in Human Molecular Biology and Genetics.

References

Abu-Issa R, Smyth G, Smoak I, Yamamura K, Meyers EN. Fgf8 is required for pharyngeal arch and cardiovascular development in the mouse. Development 2002;129:4613–4625. [PubMed: 12223417]

Arman E, Haffner-Krausz R, Chen Y, Heath JK, Lonai P. Targeted disruption of fibroblast growth factor (FGF) receptor 2 suggests a role for FGF signaling in pregastrulation mammalian development. Proc. Natl. Acad. Sci. USA 1998;95:5082–5087. [PubMed: 9560232]

Armstrong EJ, Bischoff J. Heart valve development: endothelial cell signaling and differentiation. Circ. Res 2004;95:459–470. [PubMed: 15345668]

Auguste P, Javerzat S, Bikfalvi A. Regulation of vascular development by fibroblast growth factors. Cell Tissue Res 2003;314:157–166. [PubMed: 12851809]

Barnett JV, Desgrosellier JS. Early events in valvulogenesis: a signaling perspective. Birth Defects Res. C Embryo Today 2003;69:58–72. [PubMed: 12768658]

Basson MA, Echevarria D, Ahn C. Petersen, Sudarov A, Joyner AL, Mason IJ, Martinez S, Martin GR. Specific regions within the embryonic midbrain and cerebellum require different levels of FGF signaling during development. Development 2008;135:889–898. [PubMed: 18216176]

Brown CB, Wenning JM, Lu MM, Epstein DJ, Meyers EN, Epstein JA. Cre-mediated excision of Fgf8 in the Tbx1 expression domain reveals a critical role for Fgf8 in cardiovascular development in the mouse. Dev. Biol 2004;267:190–202. [PubMed: 14975726]

Buckingham M, Meilhac S, Zaffran S. Building the mammalian heart from two sources of myocardial cells. Nat. Rev. Genet 2005;6:826–835. [PubMed: 16304598]

Camenisch TD, Schroeder JA, Bradley J, Klewer SE, McDonald JA. Heart-valve mesenchyme formation is dependent on hyaluronan-augmented activation of ErbB2-ErbB3 receptors. Nat. Med 2002;8:850–855. [PubMed: 12134143]

Danielian PS, Muccino D, Rowitch DH, Michael SK, McMahon AP. Modification of gene activity in mouse embryos in utero by a tamoxifen-inducible form of Cre recombinase. Curr. Biol 1998;8:1323–1326. [PubMed: 9843687]

de Launoit Y, Baert JL, Chotteau-Lelievre A, Monte D, Coutte L, Mauen S, Firlej V, Degerny C, Verreman K. The Ets transcription factors of the PEA3 group: transcriptional regulators in metastasis. Biochim. Biophys. Acta 2006;1766:79–87. [PubMed: 16546322]

Deng CX, Wynshaw-Boris A, Shen MM, Daugherty C, Ornitz DM, Leder P. Murine FGFR-1 is required for early postimplantation growth and axial organization. Genes Dev 1994;8:3045–3057. [PubMed: 8001823]

Engleka KA, Gitler AD, Zhang M, Zhou DD, High FA, Epstein JA. Insertion of Cre into the Pax3 locus creates a new allele of Splotch and identifies unexpected Pax3 derivatives. Dev. Biol 2005;280:396–406. [PubMed: 15882581]

Frank DU, Fotheringham LK, Brewer JA, Muglia LJ, Tristani-Firouzi M, Capecchi MR, Moon AM. An Fgf8 mouse mutant phenocopies human 22q11 deletion syndrome. Development 2002;129:4591–4603. [PubMed: 12223415]

Frank DU, Elliott SA, Park EJ, Hammond J, Saijoh Y, Moon AM. System for inducible expression of cre-recombinase from the Foxa2 locus in endoderm, notochord, and floor plate. Dev. Dyn 2007;236:1085–1092. [PubMed: 17304540]

Grove EA, Tole S, Limon J, Yip L, Ragsdale CW. The hem of the embryonic cerebral cortex is defined by the expression of multiple Wnt genes and is compromised in Gli3-deficient mice. Development 1998;125:2315–2325. [PubMed: 9584130]

Hanafusa H, Torii S, Yasunaga T, Nishida E. Sprouty1 and Sprouty2 provide a control mechanism for the Ras/MAPK signalling pathway. Nat. Cell Biol 2002;4:850–858. [PubMed: 12402043]

High F, Epstein JA. Signalling pathways regulating cardiac neural crest migration and differentiation. Novartis Found. Symp 2007;283:152–161. [PubMed: 18300420]discussion 161-164, 238-241

Hutson MR, Zhang P, Stadt HA, Sato AK, Li YX, Burch J, Creazzo TL, Kirby ML. Cardiac arterial pole alignment is sensitive to FGF8 signaling in the pharynx. Dev. Biol 2006;295:486–497. [PubMed: 16765936]

Ilagan R, Abu-Issa R, Brown D, Yang YP, Jiao K, Schwartz RJ, Klingensmith J, Meyers EN. Fgf8 is required for anterior heart field development. Development 2006;133:2435–2445. [PubMed: 16720880]

Jiang X, Rowitch DH, Soriano P, McMahon AP, Sucov HM. Fate of the mammalian cardiac neural crest. Development 2000;127:1607–1616. [PubMed: 10725237]

Karaulanov E, Knochel W, Niehrs C. Transcriptional regulation of BMP4 synexpression in transgenic Xenopus. EMBO J 2004;23:844–856. [PubMed: 14963489]

Kirby, ML. Cardiac Development. Oxford University Press; Oxford, UK: 2006.

Kisanuki YY, Hammer RE, Miyazaki J, Williams SC, Richardson JA, Yanagisawa M. Tie2-Cre transgenic mice: a new model for endothelial cell-lineage analysis in vivo. Dev. Biol 2001;230:230–242. [PubMed: 11161575]

Klaus A, Saga Y, Taketo MM, Tzahor E, Birchmeier W. Distinct roles of Wnt/beta-catenin and Bmp signaling during early cardiogenesis. Proc. Natl. Acad. Sci. USA 2007;104:18531–18536. [PubMed: 18000065]

Liu W, Selever J, Wang D, Lu MF, Moses KA, Schwartz RJ, Martin JF. Bmp4 signaling is required for outflow-tract septation and branchial-arch artery remodeling. Proc. Natl. Acad. Sci. USA 2004;101:4489–4494. [PubMed: 15070745]

Lobe CG, Koop KE, Kreppner W, Lomeli H, Gertsenstein M, Nagy A. Z/AP, a double reporter for cre-mediated recombination. Dev. Biol 1999;208:281–292. [PubMed: 10191045]

Ma C, Rong Y, Radiloff DR, Datto MB, Centeno B, Bao S, Cheng AW, Lin F, Jiang S, Yeatman TJ, et al. Extracellular matrix protein {beta}ig-h3/TGFBI promotes metastasis of colon cancer by enhancing cell extravasation. Genes Dev 2008;22:308–321. [PubMed: 18245446]

Ma L, Lu MF, Schwartz RJ, Martin JF. Bmp2 is essential for cardiac cushion epithelial-mesenchymal transition and myocardial patterning. Development 2005;132:5601–5611. [PubMed: 16314491]

Macatee TL, Hammond BP, Arenkiel BR, Francis L, Frank DU, Moon AM. Ablation of specific expression domains reveals discrete functions of ectoderm- and endoderm-derived FGF8 during cardiovascular and pharyngeal development. Development 2003;130:6361–6374. [PubMed: 14623825]

Macri L, Silverstein D, Clark RA. Growth factor binding to the pericellular matrix and its importance in tissue engineering. Adv. Drug Deliv. Rev 2007;59:1366–1381. [PubMed: 17916397]

Marguerie A, Bajolle F, Zaffran S, Brown NA, Dickson C, Buckingham ME, Kelly RG. Congenital heart defects in Fgfr2-IIIb and Fgf10 mutant mice. Cardiovasc. Res 2006;71:50–60. [PubMed: 16687131]

Moon AM, Guris DL, Seo JH, Li L, Hammond J, Talbot A, Imamoto A. Crkl deficiency disrupts fgf8 signaling in a mouse model of 22q11 deletion syndromes. Dev. Cell 2006;10:71–80. [PubMed: 16399079]

Park EJ, Ogden LA, Talbot A, Evans S, Cai CL, Black BL, Frank DU, Moon AM. Required, tissue-specific roles for Fgf8 in outflow tract formation and remodeling. Development 2006;133:2419–2433. [PubMed: 16720879]

Park EJ, Sun X, Nichol P, Saijoh Y, Martin JF, Moon AM. System for tamoxifen-inducible expression of cre-recombinase from the Foxa2 locus in mice. Dev. Dyn 2008;237:447–453. [PubMed: 18161057]

Prall OW, Menon MK, Solloway MJ, Watanabe Y, Zaffran S, Bajolle F, Biben C, McBride JJ, Robertson BR, Chaulet H, et al. An Nkx2-5/Bmp2/Smad1 negative feedback loop controls heart progenitor specification and proliferation. Cell 2007;128:947–959. [PubMed: 17350578]

Presta M, Dell'Era P, Mitola S, Moroni E, Ronca R, Rusnati M. Fibroblast growth factor/fibroblast growth factor receptor system in angiogenesis. Cytokine Growth Factor Rev 2005;16:159–178. [PubMed: 15863032]

Raible F, Brand M. Tight transcriptional control of the ETS domain factors Erm and Pea3 by Fgf signaling during early zebrafish development. Mech. Dev 2001;107:105–117. [PubMed: 11520667]

Richarte AM, Mead HB, Tallquist MD. Cooperation between the PDGF receptors in cardiac neural crest cell migration. Dev. Biol 2007;306:785–796. [PubMed: 17499702]

Roehl H, Nusslein-Volhard C. Zebrafish pea3 and erm are general targets of FGF8 signaling. Curr. Biol 2001;11:503–507. [PubMed: 11413000]

Saga Y, Miyagawa-Tomita S, Takagi A, Kitajima S, Miyazaki J, Inoue T. MesP1 is expressed in the heart precursor cells and required for the formation of a single heart tube. Development 1999;126:3437–3447. [PubMed: 10393122]

Saga Y, Kitajima S, Miyagawa-Tomita S. Mesp1 expression is the earliest sign of cardiovascular development. Trends Cardiovasc. Med 2000;10:345–352. [PubMed: 11369261]

Soriano P. Generalized lacZ expression with the ROSA26 Cre reporter strain. Nat. Genet 1999;21:70–71. [PubMed: 9916792]

Stottmann RW, Choi M, Mishina Y, Meyers EN, Klingensmith J. BMP receptor IA is required in mammalian neural crest cells for development of the cardiac outflow tract and ventricular myocardium. Development 2004;131:2205–2218. [PubMed: 15073157]

Sun X, Meyers EN, Lewandoski M, Martin GR. Targeted disruption of Fgf8 causes failure of cell migration in the gastrulating mouse embryo. Genes Dev 1999;13:1834–1846. [PubMed: 10421635]

Sun X, Mariani FV, Martin GR. Functions of FGF signalling from the apical ectodermal ridge in limb development. Nature 2002;418:501–508. [PubMed: 12152071]

Todorovic V, Frendewey D, Gutstein DE, Chen Y, Freyer L, Finnegan E, Liu F, Murphy A, Valenzuela D, Yancopoulos G, et al. Long form of latent TGF-beta binding protein 1 (Ltbp1L) is essential for cardiac outflow tract septation and remodeling. Development 2007;134:3723–3732. [PubMed: 17804598]

Trokovic R, Trokovic N, Hernesniemi S, Pirvola U, Weisenhorn D. M. Vogt, Rossant J, McMahon AP, Wurst W, Partanen J. FGFR1 is independently required in both developing mid- and hindbrain for sustained response to isthmic signals. EMBO J 2003;22:1811–1823. [PubMed: 12682014]

Vincentz JW, McWhirter JR, Murre C, Baldini A, Furuta Y. Fgf15 is required for proper morphogenesis of the mouse cardiac outflow tract. Genesis 2005;41:192–201. [PubMed: 15789410]

Waldo K, Zdanowicz M, Burch J, Kumiski DH, Stadt HA, Godt RE, Creazzo TL, Kirby ML. A novel role for cardiac neural crest in heart development. J. Clin. Invest 1999;103:1499–1507. [PubMed: 10359559]

Waldo KL, Kumiski DH, Wallis KT, Stadt HA, Hutson MR, Platt DH, Kirby ML. Contoruncal myocardium arises from a secondary heart field. Development 2001;128:3179–3188. [PubMed: 11688566]

Weinstein M, Xu X, Ohyama K, Deng CX. FGFR-3 and FGFR-4 function cooperatively to direct alveogenesis in the murine lung. Development 1998;125:3615–3623. [PubMed: 9716527]

Wurthner JU, Frank DB, Felici A, Green HM, Cao Z, Schneider MD, McNally JG, Lechleider RJ, Roberts AB. Transforming growth factor-beta receptor-associated protein 1 is a Smad4 chaperone. J. Biol. Chem 2001;276:19495–19502. [PubMed: 11278302]

Xu H, Morishima M, Wylie JN, Schwartz RJ, Bruneau BG, Lindsay EA, Baldini A. Tbx1 has a dual role in the morphogenesis of the cardiac outflow tract. Development 2004;131:3217–3227. [PubMed: 15175244]

Xu X, Qiao W, Li C, Deng CX. Generation of Fgfr1 conditional knockout mice. Genesis 2002;32:85–86. [PubMed: 11857785]

Yu K, Xu J, Liu Z, Sosic D, Shao J, Olson EN, Towler DA, Ornitz DM. Conditional inactivation of FGF receptor 2 reveals an essential role for FGF signaling in the regulation of osteoblast function and bone growth. Development 2003;130:3063–3074. [PubMed: 12756187]

Zhang J, Lin Y, Zhang Y, Lan Y, Lin C, Moon AM, Schwartz RJ, Martin JF, Wang F. Frs2α-deficiency in cardiac progenitors disrupts a subset of FGF signals required for outflow tract morphogenesis. Development 2008;135:3611–3622. [PubMed: 18832393]

Zhang X, Ibrahimi OA, Olsen SK, Umemori H, Mohammadi M, Ornitz DM. Receptor specificity of the fibroblast growth factor family. The complete mammalian FGF family. J. Biol. Chem 2006;281:15694–15700. [PubMed: 16597617]

Zhang Z, Huynh T, Baldini A. Mesodermal expression of Tbx1 is necessary and sufficient for pharyngeal arch and cardiac outflow tract development. Development 2006;133:3587–3595. [PubMed: 16914493]

Zhou W, Lin L, Majumdar A, Li X, Zhang X, Liu W, Etheridge L, Shi Y, Martin J, Van de Ven W, et al. Modulation of morphogenesis by noncanonical Wnt signaling requires ATF/CREB family-

mediated transcriptional activation of TGFbeta2. Nat. Genet 2007;39:1225–1234. [PubMed: 17767158]

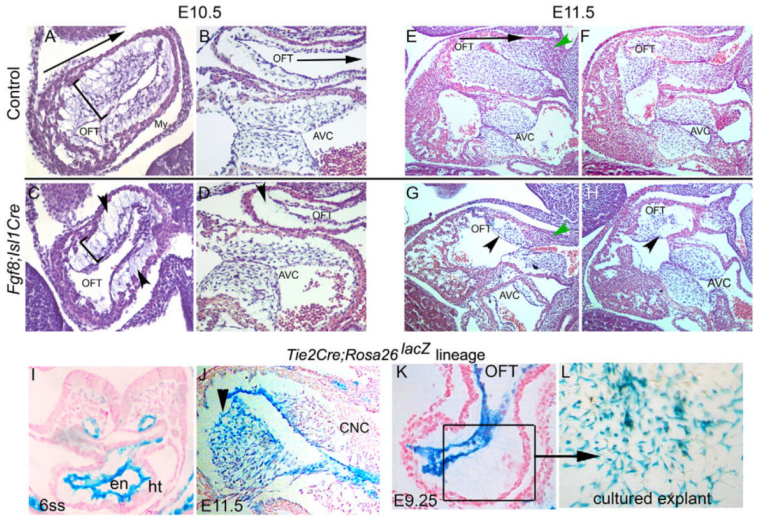

Fig. 1. Mouse OFT cushion morphogenesis is disrupted in *Fgf8$^{c/-}$;Isl1Cre* mutants

Fgf8$^{c/-}$;Isl1Cre mutants are labeled as *Fgf8;Isl1Cre*. (**A**) Transverse section across the proximal outflow tract (OFT) of a E10.5 control embryo shows many mesenchymal cells in a thick layer of cardiac jelly (bracket) lining the myocardium (My). The arrow points from proximal (close to right ventricle) to distal OFT. (**B**) Sagittal section spanning the OFT and atrioventricular canal (AVC) cushions of E10.5 control embryo. (**C**) Transverse section across the proximal OFT of an E10.5 *Fgf8;Isl1Cre* mutant embryo reveals hypoplastic cushions (arrowheads) with few mesenchymal cells in a thin layer of cardiac jelly (bracket). (**D**) Sagittal section of the OFT and AVC of an E10.5 *Fgf8;Isl1Cre* mutant with hypocellular OFT cushions (arrowhead) but normal AVC cushions. (**E**,**F**) Sagittal sections of an E11.5 control embryo shows mesenchymal cells throughout the OFT cushions. (**G**,**H**) Sagittal sections of E11.5 *Fgf8;Isl1Cre* mutants with hypoplastic proximal (black arrowhead) and distal (green arrowhead) OFT cushions. (**I**) Section through the heart (ht) of an X-Gal-stained 6-somite stage (6ss) *Rosa26^{lacZ};Tie2Cre* embryo. (**J**) Section of proximal OFT cushion (arrowhead) of an E11.5 *Rosa26^{lacZ};Tie2Cre* embryo. All of the cells in the proximal cushion are stained and the distal cushion contains unstained CNC. (**K**) Section of an E9.25 *Rosa26^{lacZ};Tie2Cre* embryo. Box encloses proximal OFT cushion. (**L**) Mesenchymal cells that invaded a collagen gel from an E9.25 *Rosa26^{lacZ};Tie2Cre* proximal OFT explant (box in K). For quantitated data, see Fig. S1 in the supplementary material.

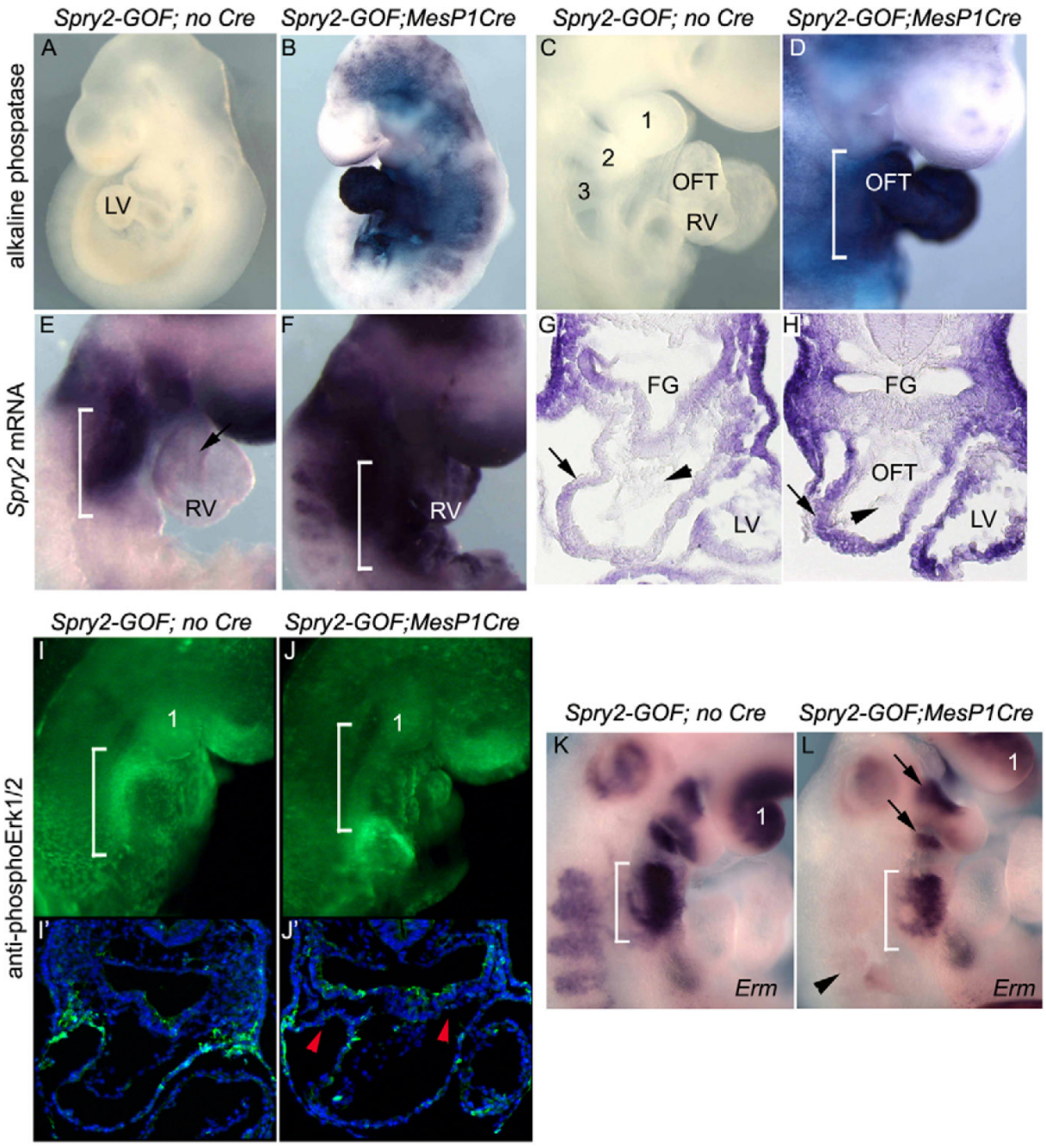

Fig. 2. Expression of *Spry2-IRES-alkaline phosphatase* in the mouse second heart field using *Mesp1Cre*

(**A-D**) Alkaline phosphatase activity is absent from control sprouty 2 gain-of-function (*Spry2-GOF*) (A,C), but present in the second heart field (SHF, white bracket) and heart tube in *Spry2-GOF;Mesp1Cre* (B,D) embryos at E9.5. Pharyngeal arches are numbered. (**E-H**) In situ hybridization for *Spry2* mRNA at E8.5 in control (E,G) and *Spry2-GOF;Mesp1Cre* (F,H) embryos, on whole-mounts (E,F) and transverse sections (G,H). White brackets indicate SHF; arrow in E points to the OFT myocardium; arrows and arrowheads in G,H indicate the OFT and unlabeled endothelial cells, respectively. (**I-J'**) Immunochemistry on E8.5 whole-mount (I,J) and sectioned (I',J') control (I,I') and *Spry2-GOF;Mesp1Cre* (J,J') embryos shows

decreased phosphoERK1/2 (pERK) staining in the SHF of mutants (white brackets in whole-mounts, red arrowheads in sections). Pharyngeal arch 1 is numbered. (**K**,**L**) In situ hybridization shows expression of *Erm* in right-sided whole-mount views of control (K) and *Spry2-GOF;Mesp1Cre* (L) embryos at E9.5. White brackets indicate SHF; arrows in L point to epithelial expression domains that are not affected (as expected); arrowhead in L indicates decreased somite expression.

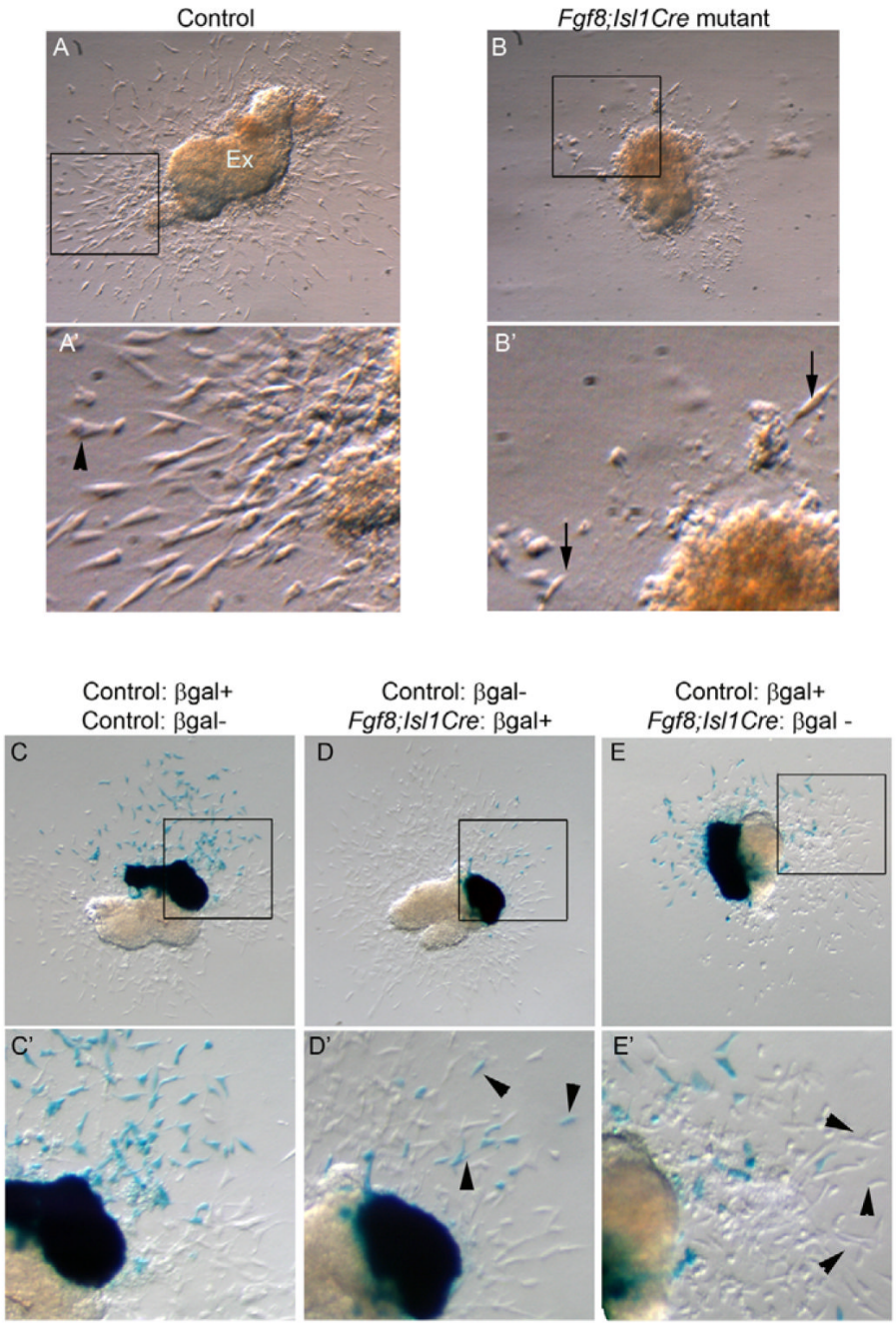

Fig. 3. Wild-type OFT myocardium rescues the endothelial-to-mesenchymal transformation defects of *Fgf8;Isl1Cre* mutants

(**A**) Explant (Ex) culture of mouse E9.5 control OFT. (**A**') Close-up of boxed region in A. Arrowhead demarcates a rare, rounded cell that migrated from the explant but failed to invade. (**B**) Explant culture of an E9.5 *Fgf8;Isl1Cre* mutant OFT reveals failure of endothelial EMT. (**B**') Close-up of boxed region in B. Arrows point to rare cells that underwent EMT. (**C**,**C**') Co-culture of E9.5 OFTs from *Rosa26^{lacZ};Isl1Cre* (blue) and controls (white). (C') Enlargement of boxed area in C. (**D**, **D**') Co-culture of control and *Fgf8;Rosa26^{lacZ};Isl1Cre* E9.5 OFTs shows rescue of mutant cells (blue, arrowheads). (D') Enlargement of boxed area in D. (**E**,**E**') Complementary experiment to D; control cells are β-galactosidase-positive (blue)

and rescued *Fgf8* mutant cells (arrowheads) are white. (E') Enlargement of boxed area in E. For quantitated data, see Fig. S2 in the supplementary material.

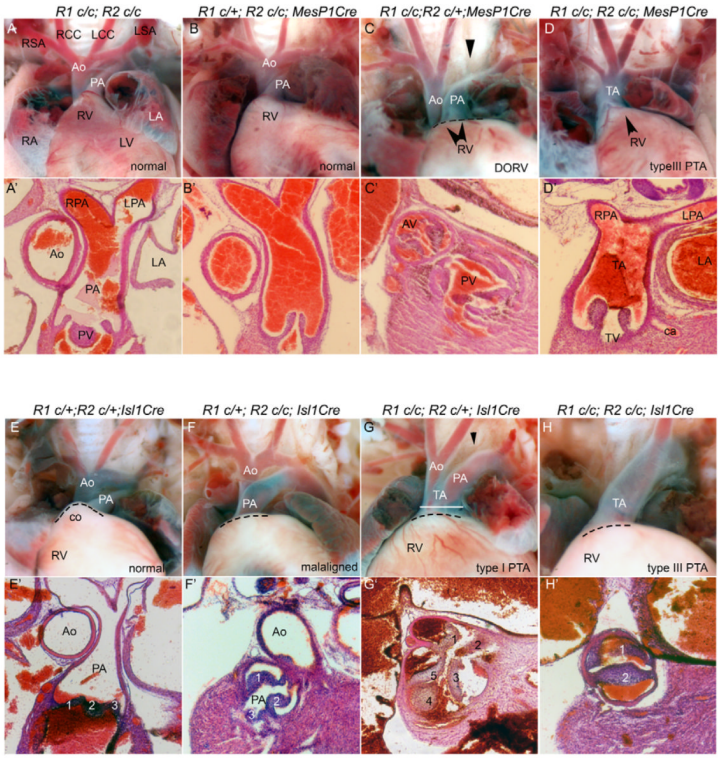

Fig. 4. OFT remodeling is sensitive to *Fgfr1/2* gene dosage in mesodermal OFT precursors and pharyngeal endoderm

Whole-mount thorax dissections (**A-H**) and sectioned preparations (**A'-H'**) of mouse embryos at E18.5. *R1, Fgfr1; R2, Fgfr2*. (A,A') Double homozygous conditional control with normal relationships of atria (LA, left atrium; RA, right atrium), ventricles (LV, left ventricle; RV, right ventricle), aorta (Ao), main pulmonary artery (PA), pulmonary valve (PV), right and left subclavian arteries (RSA, LSA) and right and left common carotid arteries (RCC, LCC). The normal shape of the RV conus (co) is indicated by the dashed line in E. These anatomic annotations are used in this and all subsequent figures. (B,B') Normal $Fgfr1^{c/+}$;$Fgfr2^{c/c}$;*Mesp1Cre* OFT. (C,C') $Fgfr1^{c/c}$;$Fgfr2^{c/+}$;*Mesp1Cre* embryo with the DORV alignment defect (double arrowhead). Hypoplasia of the RV conus (dashed line) causes the aortic valve (AV) and PV to be abnormally located in the same plane (C'). The aortic arch is interrupted (arrowhead). (D,D') $Fgfr1^{c/c}$;$Fgfr2^{c/c}$;*Mesp1Cre* embryo with type III PTA: the aortic arch and left and right branch pulmonary arteries (LPA, RPA) arise from the unseptated truncus arteriosus (TA). The truncal valve (TV) is committed to the RV (arrowhead). ca, coronary artery. (E,E') Normal OFT in an $Fgfr1^{c/+}$;$Fgfr2^{c/+}$;*Isl1Cre* double heterozygote. (F,F') $Fgfr1^{c/+}$;$Fgfr2^{c/c}$;*Isl1Cre* mutant with conal hypoplasia (dashed line) and misaligned Ao and PA. (G,G') $Fgfr1^{c/c}$;$Fgfr2^{c/+}$;*Isl1Cre*, type I PTA with pentacuspid TV (G') and interrupted aortic arch (arrowhead). (H,H') $Fgfr1^{c/c}$;$Fgfr2^{c/c}$;*Isl1Cre* mutants have type III PTA. This TV is bicuspid and arises from the RV (H').

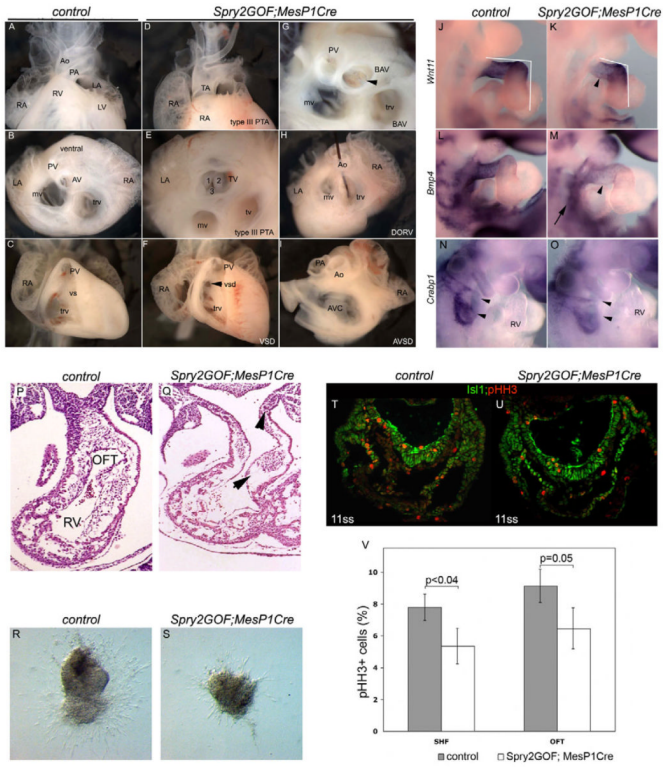

Fig. 5. Antagonism of FGF signaling by overexpression of *Spry2* disrupts OFT development

(**A-I**) Isolated E18.5 mouse hearts from controls (A-C) and *Spry2-GOF;Mesp1Cre* mutants (D-I). (A) Frontal view. (B) Superior view, ventral surface at top; the AV is dorsal and right of the PV. trv, tricuspid valve; mv, mitral valve. (C) Frontal view; RV wall removed to show PV and ventricular septum (VS). (D) Frontal view of type III PTA. (E) Superior view of embryo in D. (F) Frontal view of membranous VSD (arrowhead). (G) Superior view showing a bicuspid aortic valve (BAV, arrowhead). (H) Superior view of mutant with DORV; probe (black line) passes abnormally from the Ao into the RV. (I) Superior view, atria removed, of atrioventricular septal defect (AVSD) with incomplete fusion of the AVC cushions. (**J-O**) mRNA in situ hybridizations of E9.5 control (J,L,N) and *Spry2-GOF;Mesp1Cre* mutant (K,M,O) embryos. Mutant OFTs are short and aberrantly angulated (white lines) and the RV is hypoplastic. (J,K) *Wnt11* transcripts are decreased in the mutant OFT. (L,M) *Bmp4* transcripts are decreased in the mutant OFT (arrowhead) and in the SHF (arrow). (N,O) *Crabp1* expression is decreased in mutant pharyngeal arch neural crest (arrowheads). (**P**,**Q**) Sections of E10.5 control (P) and *Spry2-GOF;Mesp1Cre* mutant (Q). Arrowhead points to reduced CNC and arrow to proximal cushion defects in the mutant. (**R**,**S**) Explant cultures of control (R) and *Spry2-GOF;Mesp1Cre* (S) OFTs show reduction in EMT when reception of FGF signaling in mesodermal cells is compromised. (**T**,**U**) Immunohistochemical detection of phosphohistone H3 (pHH3, red) and Isl1 (green) in E8.5 [11-somite stage (ss)] embryos. (**V**) Quantitation of $pHH3^{+}$ cells as a percentge of the total number of cells in the SHF and OFT of E8.5 (10-11ss) control and *Spry2-GOF;Mesp1Cre* mutants. Proliferation is significantly decreased in both tissues (SHF, P=0.039; OFT, P=0.05). Three sections per embryo were counted and n=3 embryos per genotype. The s.d. was measured with Student's t-test.

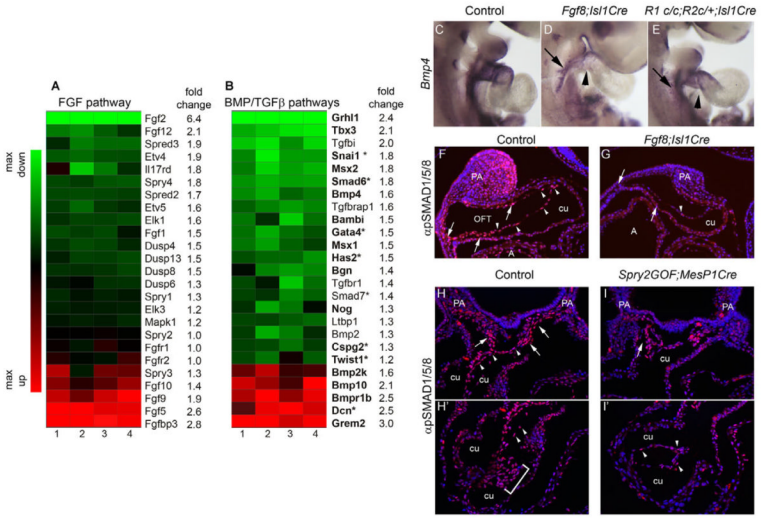

Fig. 6. Loss of FGF8 signaling in the SHF and pharyngeal endoderm disrupts BMP and TGFβ signaling

(**A**,**B**) Intensity maps of relative expression of members and targets of the FGF and BMP/TGFβ signaling pathways obtained from four Agilent microarrays comparing *Fgf8;Isl1Cre* mutant to control OFTs. Red indicates increased expression and green decreased expression in mutants. Note the reproducible direction and magnitude of the changes. In the BMP/TGFβ gene list, BMP pathway members are in bold, TGFβ pathway members are in regular type and shared genes are marked with an asterisk. Fold changes are log base 2; $P<0.05$. (**C-E**) mRNA in situ hybridizations of E9.5 control and *Fgf8;Isl1Cre* mutants. *Bmp4* expression is decreased in the OFT (arrowhead) and SHF (arrow) of (D) *Fgf8;Isl1Cre* and (E) *Fgfr1*$^{c/c}$*;Fgfr2*$^{c/+}$*;Isl1Cre* mutants that develop PTA. (**F**,**G**) Anti-phosphoSMAD1/5/8 immunohistochemistry on sagittal sections of control versus *Fgf8;Isl1Cre* mutant OFTs. Hoechst staining in blue, anti-pSMAD in red. pSMAD^{+} cells are abundant in control, compared with mutant, pharyngeal and subendothelial mesenchyme (arrows) and in the OFT endothelium (arrowheads). cu, proximal OFT cushion; PA, pharyngeal arch. (**H-I**') Anti-phosphoSMAD1/5/8 immunohistochemistry on transverse sections of control versus *Spry2-GOF;Mesp1Cre* mutant OFTs. Hoechst staining in blue, anti-pSMAD in red. pSMAD^{+} cells are abundant in control OFT endothelium (arrowheads) and in subendothelial mesenchymal cells (arrows). (H,I) Distal OFT cushions (cu). (H',I') Proximal OFT cushions. Bracket in H' shows large numbers of pSMAD^{+} endothelial cells in the control.

Table 1

Incidence of OFT malformations after ablation of *Fgfr1/2* with *Mesp1Cre* or *Isl1Cre*, or activation of *Spry2-GOF* with *Mesp1Cre*

Fgfr1/2* ablation with *Mesp1Cre

	No *Cre*					Mesp1Cre				
Fgfr1;Fgfr2	**c/c;+/+***	**c/+;c/+**	**c/+;c/c**	**c/c;c/+**	**c/c;c/c**	**c/c;+/+***	**c/+;c/+**	**c/+;c/c**	**c/c;c/+**	**c/c;c/c**
Normal	14	9	31	4	14	12	19	9	8	
Alignment						2‡			7 DORV	
PTA type I										
PTA type III										4††
VSD								1§	8¶	4
BAV						ND			4**	1
ASD								1	1	1
n	14	9	31	4	14	14	18	10	18	5
Expected *n*†	14	5	20	5	20	14	18	7	18	7

Fgfr1/2* ablation with *Isl1Cre

	No *Cre*					*Isl1Cre*				
Fgfr1;Fgfr2	**c/c;+/+***	**c/+;c/+**	**c/+;c/c**	**c/c;c/+**	**c/c;c/c**	**c/c;+/+***	**c/+;c/+**	**c/+;c/c**	**c/c;c/+**	**c/c;c/c**
Normal	20	13	11	11	8	7	15		2	
Alignment						2‡‡		4§§		
PTA type I								1	6	
PTA type III									2	5
VSD						6¶¶			9	5
BAV						4			3***	
ASD					1	2				3
n	20	13	11	11	8	14	15	5	13	5
Expected *n*	18	11	11	11	11	18	11	11	11	11

Activation of *Spry2-GOF* with *Mesp1Cre*

	Spry2-GOF;Mesp1Cre	
	Control	**Mutant**
Normal	19	3
Alignment		3
PTA type I		1
PTA type III		2
VSD		9
BAV		4
AVCD		5
n	19	13

Note that the total number of defects exceeds *n* because specimens have more than one defect.

+, wild-type allele; c, conditional allele.

ND, not determined.

[*] *Fgfr1* single-mutant analyses obtained from separate breedings.

[†] *Mesp1* and *Fgfr2* linkage results in non-Mendelian distribution.

[‡] One TGA, one DORV.

[§] Inlet VSD (ventricular septal defect).

[¶] Seven with DORV, one with BAV (bicuspid aortic valve).

[**] Two isolated, one with VSD, one with DORV.

[††] One with atrioventricular canal defect (AVCD).

[‡‡] One TGA, one DORV.

[§§] Two DORV, two posteriorly rotated aorta.

[¶¶] Three associated with OFT defects, three with BAV.

[***] All associated with VSD.